Compensation of the Secondary Voltage of a CCVT Considering Hysteresis Characteristics of the Core in Time Domain

Yong-Cheol Kang, Taiying Zheng, Yeon-Hee Kim, Sung-Il Jang, and Yong-Gyun Kim

   Abstract-This paper proposes an algorithm for compensating the distorted secondary voltage of a coupling capacitor voltage transformer (CCVT) in the time domain considering the hysteresis characteristics of a core. The voltage across the capacitor and the tuning reactor is the error between the correct primary voltage and the measured primary voltage. The proposed algorithm estimates and adds the voltage across the capacitor and the reactor to the measured primary voltage to obtain the correct voltage considering the effect of the hysteresis characteristics of the core. The algorithm reduces the errors significantly both in the steady state and during the fault. The performance of the algorithm is verified under the various fault conditions by varying the fault distance, the fault inception angle and the fault impedance with the EMTP generated data. Test results clearly indicate that the algorithm can increase the accuracy of a CCVT significantly under the fault conditions as well as in the steady state. The algorithm may improve the performance of a relay or a metering device.

   Keywords: CCVT, compensation, hysteresis, time domain.

I. INTRODUCTION

I N an extra high voltage or ultra high voltage system, the voltage is too high to measure using a voltage transformer (VT) because of insulation and costs. Thus, a coupling capacitor voltage transformer (CCVT) has been widely used to obtain the standard low voltage signals for protection and measurement. There is a resonance between the capacitor voltage divider and the tuning reactor in the steady state, which is designed based on the power system frequency to avoid the phase angle shift. The resonance will reduce the errors between the correct voltage and the measured voltage [1]. However, the errors still exist in the measured voltage

due to the hysteresis characteristics of the core.

   Moreover, if the resonance is broken by the disturbances, the errors will also increase. For example, when a fault occurs, dc offset and harmonic components are generated as well as the power system frequency component. These transient components break the resonance, which cause some errors in the measured voltage of the CCVT. The protection relays using the voltage may mal-operate or be delayed. Many researches have been reported [2]–[6] to study the performance of a CCVT and minimize the negative influence of the transients caused by the instrument transformer. These papers describe the detailed model of a CCVT.

   The compensation for the distorted voltage in the fault conditions is necessary to reduce the errors. A dynamic compensation method [7] using the transfer functions of a CCVT was proposed. The algorithm removes the CCVT induced transients from the voltage signal based on inversion of the CCVT simplified transfer function. Since the analysis was based on frequency domain, non-linear characteristics of the core were not included and the errors in the measured voltage are contained even in the steady state. The parameters of the step-down transformer were neglected to reduce the computation burden. Since such simplification also generates the errors because of the voltage drop upon them, it is essential to compensate the distorted secondary voltage in real time.

   This paper proposes an algorithm for compensating the distorted secondary voltage of the CCVT in the time domain considering the hysteresis characteristics of the core. From the measured secondary voltage of the CCVT, the secondary current and voltages of the VT are obtained. The primary voltage and current of the VT are calculated considering the turns ratio of the VT and the effects of the hysteresis characteristics. The voltage across the capacitor and the tuning reactor, which is the difference between the correct primary voltage and the measured primary voltage of the CCVT, is obtained and added to the measured primary voltage. The proposed algorithm removes the effect of the hysteresis characteristics of the core and reduces the errors between the primary and secondary voltages both in the steady state and during the fault. The performance of the algorithm is verified under not only the various fault conditions by varying the fault distance, the fault inception angle and the fault impedance, but also steady state ones with the EMTP generated data.

II. Compensating Algorithm

A. Compensating Algorithm in the Time Domain

To cope with the drawback of the algorithm [7], this paper proposes a compensating algorithm of the distorted secondary voltage in the time domain. It can deal with the problem of hysteresis characteristics of a core and make the calculation simple.

Fig. 1 shows the adopted CCVT model, which consists of:
- the capacitor voltage divider (C_1, C_2),
- the tuning reactor (L, R),
- the step-down transformer (L_{T1}, R_{T1}, L_{T2} and R_{T2}) with an equivalent tray capacitance (C_{T1}) included at the primary winding and the non-linear exciting branch, and
- the ferro-resonance suppression circuit (*FSC*) and the CCVT load: L_1, R_1, R_2, R_0 and L_0.

In this model, all necessary parameters of the step-down voltage transformer were not neglected.

Applying Thévénin transform to the capacitor voltage divider, the CCVT's Thévénin equivalent circuit is shown in Fig. 2. e_{th} and C are the Thévénin source and the Thévénin equivalent impedance, respectively. C is given by

$$C = C_1 + C_2. \tag{1}$$

B. The Secondary Side Branch:

In Fig. 2, $i_B(t)$, flowing through the burden of the CCVT, can be obtained by integrating:

$$v_B(t) = R_0 i_B(t) + L_0 \frac{di_B(t)}{dt} \tag{2}$$

where $v_B(t)$ is the voltage across the burden, which can be measured directly.

Applying KVL and KCL in the secondary side of the VT yields, the voltage $v_{VT2}(t)$ and the current $i_{VT2}(t)$ of the secondary side of VT can be calculated as:

$$v_{VT2}(t) = v_{RT2}(t) + v_B(t) \tag{3}$$

$$i_{VT2}(t) = i_{L1}(t) + i_{R1}(t) + i_{R2}(t) + i_B(t) \tag{4}$$

where, $v_{RT2}(t)$ is the voltage across the secondary winding resistance and leakage inductance, and $i_{L1}(t)$, $i_{R1}(t)$ and $i_{R2}(t)$ are the currents flowing through three parts of the *FSC*, respectively. They can be calculated easily from $v_B(t)$ and $i_B(t)$.
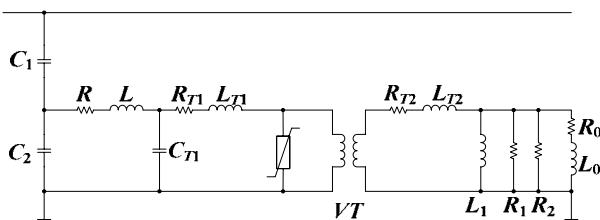

Fig. 1 Adopted CCVT model.

C. The Ideal Voltage Transformer:

The primary voltage and current of the VT can be obtained considering the turns ratio of the VT, i.e.:

$$v_{VT1}(t) = v_{VT2}(t) \cdot N_1 / N_2 \tag{5}$$

$$i_{VT1}(t) = i_{VT2}(t) \cdot N_2 / N_1 \tag{6}$$

where, N1 and N2 are the number of the turns of the primary and secondary windings of the VT, respectively.

D. The Exciting Branch:

Many of the models [8]–[9] developed for representing flux-current variations in transformer cores have been based purely on the magnetizing characteristic, and other models [10]–[11] have considered magnetic excursions from the parent loop, but these lacked the simplicity so that they may not compensate the distorted secondary voltage in real time.

When a CCVT is energized in the steady state, magnetizing trajectory is on the major loop. However, when a fault occurs, the magnetizing trajectory deviates from the major loop. In most cases, it is more likely on a trajectory of minor loops. Therefore, it is a key step to obtain the minor loops during the fault.

The flow chart is shown in Fig. 3. From (5), as the voltage across the exciting branch can be estimated, the core flux $\lambda(t)$ can be estimated as:

$$\lambda(t) = \int_{t-\Delta t}^{t} v_{VT1}(t) dt + \lambda(t - \Delta t) \tag{7}$$

where the initial value of the core flux can be estimated using one cycle data of the flux. Then, using the hysteresis loops, the exciting current can be estimated.

E. The Secondary Side Branch:

The current flowing through the winding resistance and leakage inductance, $i_{RT1}(t)$, can be estimated as:

$$i_{RT1}(t) = i_{VT1}(t) + i_e(t). \tag{8}$$

Applying KVL and KCL in the primary side of the VT yields, the Thévénin voltage, $e_{th}(t)$, can be calculated as:

$$e_{th}(t) = v_{CRL}(t) + v_{RT1}(t) + v_{VT1}(t) \tag{9}$$

where, $v_{CRL}(t)$ is the voltage across the Thévénin equivalent impedance and the tuning reactor, and $v_{RT1}(t)$ is the voltage across the primary winding resistance and leakage inductance. They can be easily calculated from $i_{RT1}(t)$.

Finally, the voltage of transmission line $v_{BUS}(t)$ is directly related with $e_{th}(t)$.

$$v_{BUS}(t) = e_{th}(t) \cdot C / C_1 \tag{10}$$

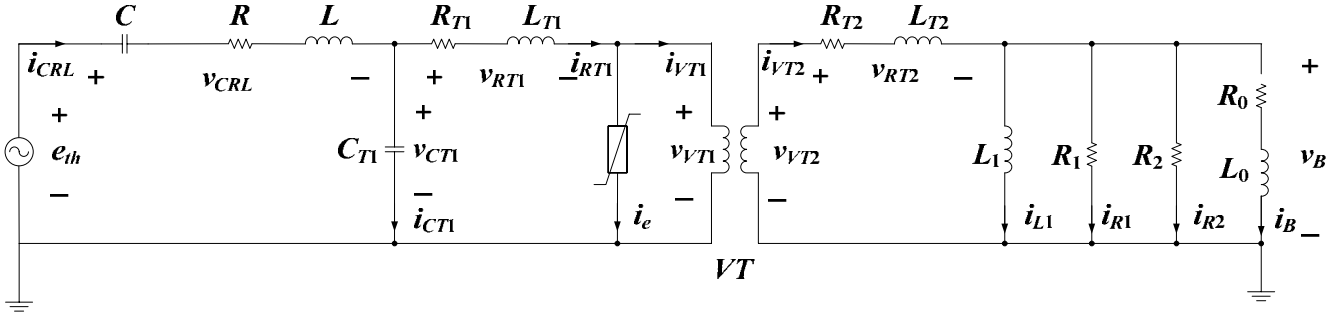With (3), (5), (9) and (10), $v_{BUS}(t)$ can be rewritten as:

Fig. 2 Thévénin equivalent circuit of the CCVT.

$$v_{BUS}(t) = (C/C_1) \cdot \begin{pmatrix} v_{CRL}(t) + v_{RT1}(t) \\ + (N1/N2) \cdot (v_{RT2}(t) + v_B(t)) \end{pmatrix} \quad (11)$$

As seen in (11), the errors of the measured primary voltage consists of three parts, which are the error generated by the capacitor voltage divider and the tuning reactor, the errors generated by the winding resistance and leakage inductance of the primary side and the secondary side.

III. CASE STUDIES

Fig. 4 shows a single-line diagram of a typical Korean 345 kV transmission system. The primary voltages and the secondary voltages are obtained using EMTP. The sampling rate is 64 samples per cycle. The signals of the secondary voltages of the CCVT are passed through anti-aliasing low-pass RC filters with the cutoff frequency of 1,920 Hz, which is half the sampling frequency.
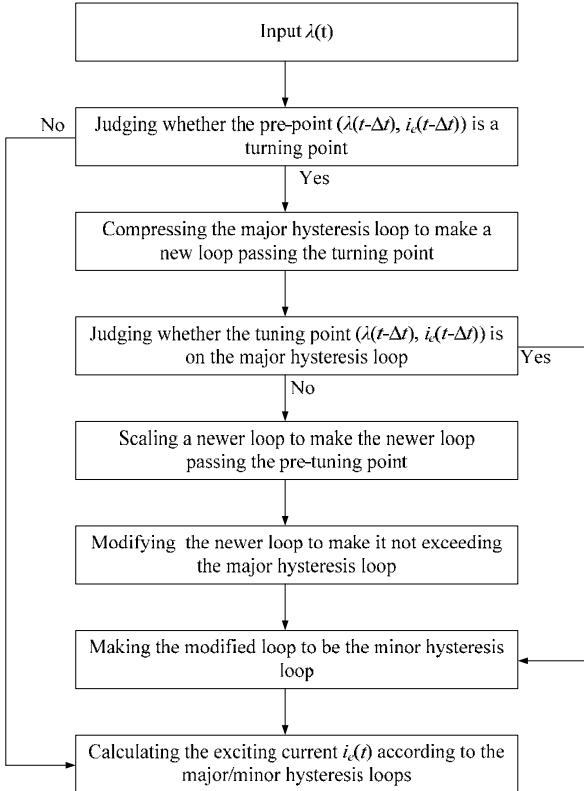

Fig. 3 Flow chart of the calculation of the exciting current.

A. Fault Inception Angle

Fault inception angle has much influence on high frequencies generated in the transmission line when a fault occurs. Thus, the algorithm was tested by varying the fault inception angle from 0° to 90°.

1) Case 1: 0 ° Fault, Three Phase-to-Ground, Fault Distance of 0.5km, and Fault Impedance of 0Ω: The fault occurs at 33ms. The measured (dotted), compensated (dashed) and correct (solid) voltages are shown in Fig. 5a. A part of Fig. 5a in the steady state is expanded and shown in Fig. 5b. The dotted and solid lines in the left part of Fig. 5b are the measured and correct voltages, respectively and those in the right part of Fig. 5b are the compensated and correct voltages. Table I shows the ratio errors and phase errors of the measured and compensated voltages. The ratio errors of the measured and compensated voltages are -0.827% and 0.028%, respectively. The phase errors of the measured and compensated are 27.7 min and -0.84 min, respectively. The proposed algorithm can increase the accuracy of the CCVT even in the steady state.
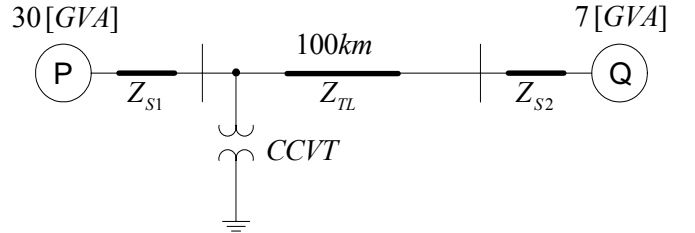

Fig. 4 Model system studied.

TABLE I
ERRORS OF THE MEASURED AND COMPENSATED VOLTAGES

	Ratio errors	Phase errors
Measured Voltages	-0.827%	27.7 Min
Compensated Voltages	0.028%	-0.84 Min

(a) Measured, compensated and correct primary voltages.

(b) Under steady state: Expanded measured and correct primary voltages (left); Expanded compensated and correct primary voltages (right).

(c) v_B, v_{RT2}, v_{RT1}, v_{CRL}, and v_{BUS}.

(d) Expanded measured and correct primary voltages.

(e) Expanded compensated and correct primary voltages.

(f) Calculated and correct exciting currents of transformer.

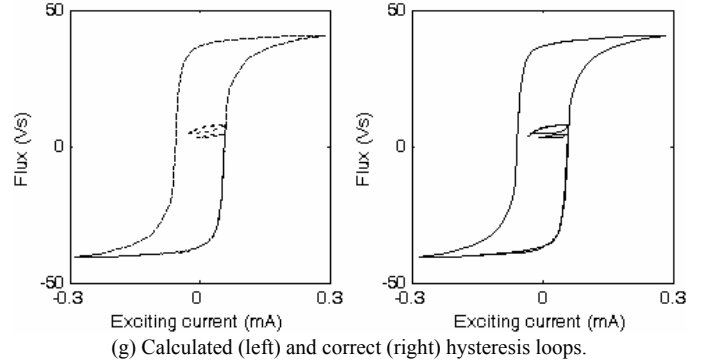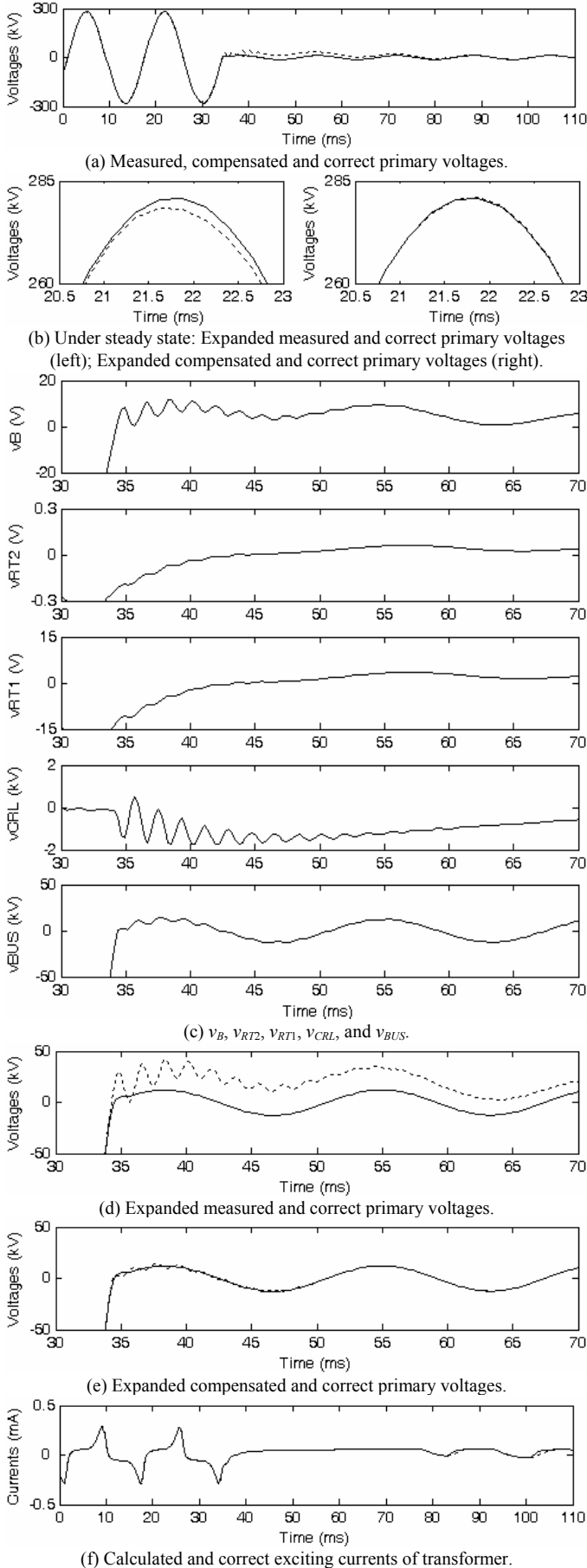(g) Calculated (left) and correct (right) hysteresis loops.
Fig. 5 Results for case 1.

Fig. 5c shows the voltages v_B, v_{RT2}, v_{RT1}, v_{CRL}, and v_{BUS}. Taking into account the effects of the transformer ratio and capacitor voltage divider, v_{BUS} can be attained by the sum of v_B, v_{RT2}, v_{RT1} and v_{CRL}. The expanded measured (dotted) and correct (solid) voltages in the transient state are shown in Fig. 5d, and the expanded compensated (dotted) and correct (solid) voltages in the transient state are shown in Fig. 5e. The difference between the measured and the correct voltages is large whilst the difference between the compensated and correct voltages is very small. The calculated (dotted) and correct (solid) exciting current of transformer are shown in Fig. 5f. The calculated (left) and correct (right) hysteresis loops are shown in Fig. 5g.

The results for this case indicate that the proposed algorithm can estimate the correct voltage accurately.

2) Case 2: 90° Fault, Three Phase-to-Ground, Fault Distance of 0.5km, Fault Impedance of 0Ω: Case 2 is the same as Case 1 except the fault inception angle is 90°. Fig. 6 shows the results for case 2. The expanded measured (dotted) and correct (solid) voltages in the transient state are shown in Fig. 6a, and the expanded compensated (dotted) and correct (solid) voltages in the transient state are shown in Fig. 6b.

As shown in Fig. 6b, compensated voltages have some errors. This is because there are errors generated in the calculation of the voltage across an inductor or the current flowing through a capacitor. While the trapezoidal rule filters out high-frequency currents in inductances connected to voltage sources, it unfortunately also amplifies high frequency voltages across inductances where currents are forced into them. This causes numerical oscillations. V. Brandwajn [12] and F. Alvarado [13] describe a method for damping these numerical oscillations with parallel damping resistances.

The proposed compensation algorithm uses the sampling rate of 64 samples per cycle (s/c). However, if higher sampling rate than 64 s/c is used, the errors are reduced significantly. Fig. 6c shows the results for the sampling rate of 128 s/c.

The results indicate that the algorithm successfully estimates the correct primary voltage irrespective of the fault inception angle.

B. Fault Distance

Fault distance affects the voltage across the transmission line between the relaying point and the fault point. Thus, the algorithm was tested by varying the fault distance from 0.5km to 50km, and the voltage after a fault was varied from 4.4% to 82.3% of the voltage prior to fault.

1) Case 3: 0 ° Fault, Three Phase-to-Ground, Fault Distance of 5km, Fault Impedance of 0Ω: Fig. 7 shows the results for Case 3; this is identical to Case 1 except for the fault distance of 10km. Comparing the results with those of Case 1, when the fault distance is long, the voltage between the relay location and the fault point does not decrease so much, and the errors of the measured voltage and the compensated voltage are smaller than those in the shorter fault distance. The results show that the proposed algorithm successfully compensates the primary voltage irrespective of the fault distance.
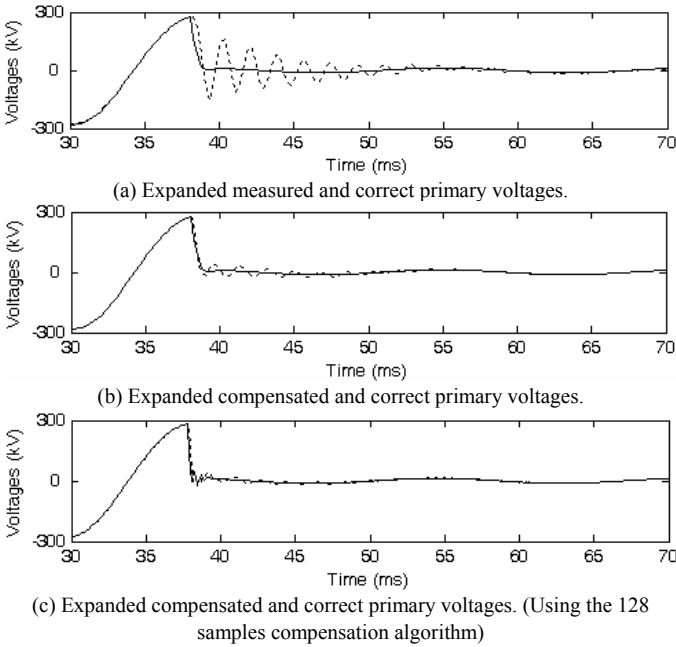

(a) Expanded measured and correct primary voltages.

(b) Expanded compensated and correct primary voltages.

(c) Expanded compensated and correct primary voltages. (Using the 128 samples compensation algorithm)

Fig. 6 Results for case 2.

(a) Expanded measured and correct primary voltages.

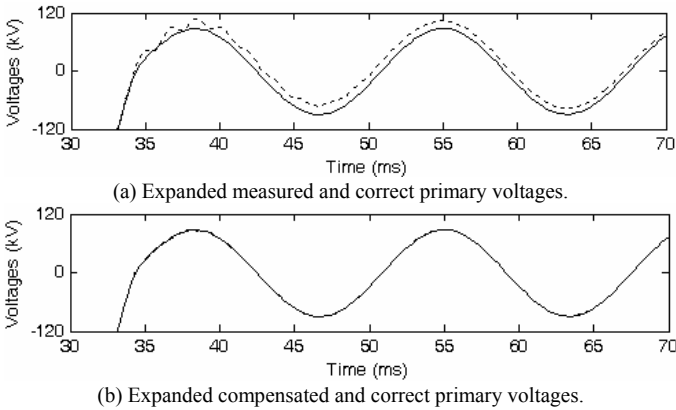(b) Expanded compensated and correct primary voltages.

Fig. 7 Results for case 3.

C. Fault Impedance

Fault impedance is another fault condition affecting the voltage across the transmission line between the relaying point and the fault point. The algorithm was tested by varying fault impedance from 0Ω to 100Ω, and the voltage after a fault was varied from 4.4% to 99.5% of the voltage prior to fault.

1) Case 4: 0 ° Fault, Three Phase-to-Ground, Fault Distance of 0.5km, Fault Impedance of 2.5Ω: Fig. 8 shows the results for Case 4; this is identical to Case 1 except for the fault impedance of 2.5Ω. Comparing the results with those of Case 1, when the fault impedance is large, the voltage between the relay location and the fault point does not decrease so much, and the errors of the measured voltage and compensated voltage are smaller than those in the smaller fault impedance.

The results show that the proposed algorithm successfully compensates the primary voltage irrespective of the fault impedance.

IV. CONCLUSIONS

This paper proposes a compensating algorithm for the secondary voltage of a CCVT in the time domain. From the measured secondary voltage, the voltage across the capacitor and the tuning reactor is estimated and added to compensate the distorted secondary voltage. The effect of the hysteresis characteristics of the core is eliminated in the proposed algorithm.

Under steady state operating conditions, the algorithm can increase the accuracy of a CCVT significantly. The performance of the algorithm was investigated on various fault conditions varying the fault inception angle, the fault distance and the fault impedance. The test results indicate that the algorithm can compensate the distorted secondary voltage of the CCVT irrespective of these fault conditions.

The algorithm can increase the accuracy of the CCVT significantly during the fault as well as in the steady state and may consequently increase the performance of the protection algorithms.
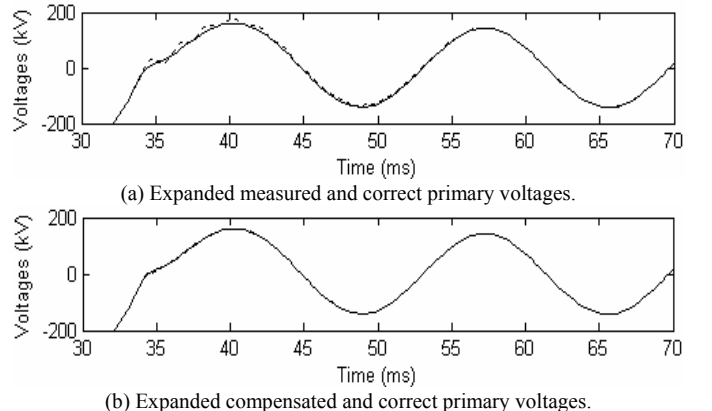

(a) Expanded measured and correct primary voltages.

(b) Expanded compensated and correct primary voltages.

Fig. 8 Results for case 4.

V. REFERENCES

[1] Stanley H. Horowitz, and Arun G. Phadke, Power system relaying, John Wiley and Sons INC, 1992, pp. 48−71.

[2] J. R. Lucas, P. G. Mclaren, W. W. L. Keerthipala, R. P. Jayasinghe, "Improved simulation models for current and voltage transformers in relay studies, " IEEE Trans. Power Delivery, Vol. 7, No.1, Jan. 1992, pp. 152−159.

[3] Working Group C-5 of the Systems Protection Subcommittee of the IEEE Power System Relaying Committee, "Mathematical Models for Current, Voltage, and Coupling Capacitor Voltage Transformers," IEEE Trans. Power Delivery, Vol. 15, No.1, Jan. 2000, pp. 62−72.

[4] M. Kezunovic, C. W. Fromen, S. L. Nilsson, "Digital models of coupling capacitor voltage transformers for protective relay transient studies, " IEEE Trans. Power Delivery, Vol. 7, No.4, Oct. 1992, pp. 1927−1935.

[5] J. R. Marti, L. R. Linares, and H. W. Dommel, "Current Transformers and Coupling-Capacitor Voltage Transformers in real-time Simulations," IEEE Trans. Power Delivery, Vol. 12, No 1, Jan. 1997, pp. 164−168.

[6] Lj. Kojovic, M. Kezunovic, C. W. Fromen, "A new method for the CCVT performance analysis using field measurements, signal processing and EMTP modeling," IEEE Trans. Power Delivery, Vol. 9, No. 4, Oct. 1994, pp. 1907−1915.

[7] J. Izykowski, B. Kasztenny, E. Rosolowski, M. M. Saha and B. Hillstrom, "Dynamic Compensation of Capacitive Voltage Transformers," IEEE Trans. Power Delivery, Vol. 13, No. 1, Jan. 1998, pp. 116−122.

[8] D. O'Kelly, "Hysteresis and eddy-current losses in steel plates with non-linear magnetization characteristics," Proc. IEE, Vol. 119, No. 11, 1972, pp. 1675−1676.

[9] G. F. T. Widger, "Representation of magnetization curves over extensive range by rational fraction approximations," Proc. IEE, Vol. 116, No. 1, Jan. 1969, pp. 156−160.

[10] Ray, S., "Digital simulation of B/H excursions for power system studies," Proc. IEE, Vol. 135, Pt C, No. 3, May. 1988, pp. 202−209.

[11] Hassani, M. M., Lachiver, G., and Jasmin, G., "Numerical simulation of the magnetic core of a transformer in transient operations," Canadian Conference on Electrical and Computer Engineering, Sept, 1989, pp. 289-291.

[12] V. Brandwajn, "Damping of numerical noise in the EMTP solution," EMTP Newsletter, Vol. 2, no. 3, Feb. 1982, pp.10−19

[13] F. Alvarado, "Eliminating numerical oscillations in trapezoidal integration, " EMTP Newsletter, Vol. 2, no. 3, Feb. 1982, pp. 20−32

Yong-Cheol Kang (S'93–M'98) received the B.S., M.S., and Ph. D degrees from Seoul National University, Seoul, Korea, in 1991, 1993, and 1997, respectively.
He is now an Associate Professor at Chonbuk National University, Chonju, Korea. His research interest is development of new protection systems for power systems using digital signal processing techniques.

Taiying Zheng (S'06) received the B. S. and M. S. degrees from Zhe Jiang University, HangZhou, China, in 2004, and Chonbuk National University, Chonju, Korea, in 2006. He is now pursuing the PhD degree at Chonbuk National University, Chonju, Korea.
His research interest is development of new protection systems for power systems using digital signal processing techniques.

Yeon-Hee Kim received the B. S. degrees from Chonbuk National University, Korea, in 2006. He is now pursuing the M.S. degree at Chonbuk National University, Korea. He has been a researcher of the Hankook IED Eng. Inc. since 2005.
His research interests include the development for electronic coupling capacit or voltage transformer (ECCVT), electronic current transformer (ECT) and ele ctronic voltage transformer (EVT).

Sung-Il Jang (S'01–M'04) received the B.S., M.S., and PhD degrees in electrical engineering from Kangwon National University, Korea, in 1996, 1998, and 2003, respectively. He was with the BK21 Research Division for Information Technology at Seoul National University, Korea for 2 years after graduate. Currently, he is now a research professor at Chonbuk National University, Chonju, Korea. His research interests include the development for electronic current transformer (ECT) and electronic voltage transformer (EVT), distributed generation interface with power system, power quality analysis, and adaptive relaying.

Yong-Kyun Kim received the B.S., degree in electrical engineering from Hong-Ik University, Korea, in 2000. He has been a president of the Hankook IED Eng. Inc. since 2005.
His research interests include the development for ECT and EVT.